Heliyon 9 (2023) e13294

Contents lists available at ScienceDirect

Heliyon

journal homepage: www.cell.com/heliyon

Research article

S100A9 promotes glycolytic activity in HER2-positive breast cancer to induce immunosuppression in the tumour microenvironment

Jia-qi Yuan, Shou-man Wang, Lei Guo *

Clinical Research Center for Breast Cancer Control and Prevention in Hunan Province, Multidisciplinary Breast Cancer Center, Department of General Surgery, Xiangya Hospital, Central South University, Changsha, Hunan Province, China

ARTICLE INFO

Keywords:
HER2-positive breast cancer
S100 calcium-binding protein A9 (S100A9)
Glycolysis
Tumour infiltrating lymphocyte
c-Myc

ABSTRACT

Purpose: The purpose of this study was to investigate the correlation between S100 calcium binding protein A9 (S100A9), tumour glycolysis and tumour infiltrating lymphocytes (TIL) in human epidermal growth factor receptor 2 (HER2) - positive breast cancer (BRCA).

Materials and methods: A total of 667 BRCA patients in Xiangya Hospital of Central South University were enrolled in this study. Haematoxylin and eosin (H&E) staining were used to count TIN in tissues. Human breast cancer cell lines (SK-BR-3 cells and BT474 cells) were transfected with S100A9 specific small interfering RNA (siRNA). The expressions of S100A9, glycolytic enzymes and lymphocyte markers were detected by immunohistochemistry (IHC) staining, Western blot and immunofluorescence. Lactate production, glucose consumption and the extracellular acidification rate (ECAR) were detected to assess glycolysis activity.

Results: S100A9 was significantly overexpressed in HER2+ cases. The expressions of phosphoglycerol kinase 1 (PGK1), lactate dehydrogenase A (LDHA) and enolase α (ENO1) were significantly up-regulated in S100A9 dominant tissues. The expressions of PGK1, LDHA and ENO1 detected in S100A9 silenced cell lines were significantly down-regulated. Moreover, S100A9 silencing significantly altered lactate production, glucose uptake and ECAR levels in HER2+ cell lines. Co-expression of S100A9 and c-Myc was detected in HER2+ tissues. The absence of S100A9 greatly hindered β-catenin expression in cell lines, which later induced the phosphorylation of c-Myc.

The amount of TILs in cases with abundant S100A9 and LDHA was much greater than in cases with low S100A9 levels and poorer LDHA. TIL deficiency and elevated S100A9 intensity are factors affecting the survival rate of HER2+ BRCA cases.

Conclusions: S100A9 overexpression upregulated the glycolysis activity of tumour cells through the c-Myc-related pathway, suppressing lymphocyte infiltration in the tumour stroma, affecting the efficacy of immune regulation and long-term survival of patients.

1. Introduction

As a special type of breast cancer (BRCA) with overexpression of the human epidermal growth factor receptor 2 (HER2) is known to

* Corresponding author.
E-mail address: GL4368@csu.edu.cn (L. Guo).

https://doi.org/10.1016/j.heliyon.2023.e13294
Received 5 November 2022; Received in revised form 19 January 2023; Accepted 26 January 2023
Available online 29 January 2023

shorten disease-free survival and overall survival [1]. Fortunately, humanised monoclonal antibodies (trastuzumab and pertuzumab) and tyrosine kinase inhibitors (lapatinib) have been widely introduced as treatment; these have significantly reduced recurrent risk and improved prognosis [2]. Nevertheless, some HER2+ BRCA cases still do not respond well to current clinical practice; thus, other factors that alter therapeutic response need to be identified [3].

Tumour cells tend to obtain energy through glycolysis, and this is known as the Warburg effect, which is considered as a hallmark of malignant diseases [4]. Excessive aerobic glycolysis resulted in lactate accumulation [5], which inhibited the activation of infiltrating $CD8^+$ T cells, thus leading to immune suppression in the tumour microenvironment (TME) [6]. Interestingly, HER2+ BRCA cells increased glycolysis activity, whereas HER2-insufficient cases relied on oxidative phosphorylation, which showed that overexpression of HER2 was typically a metabolic phenotype [7]. The level of tumour-infiltrating lymphocytes (TILs) in HER2 BRCA was similar to that in triple negative BRCA (TNBC), which was widely demonstrated to be a lymphocyte-dominant breast cancer. Thus, glycolysis-related immune suppression of TME of HER2+ BRCA should be carefully studied [8]. However, few reports have focused on this field.

Some unfavourable factors in the TME weakened the anti-tumour immune, thus contributing to the tumour progression. Stromal extracellular matrix (ECM) proteins released cancer cells from the immune surveillance. Cancer cells also employed the immune checkpoints to obtain immune evasion. As one of the most essential immune checkpoints, PD-1/PD-L1 interaction led to a series of negative co-stimulatory events, such as increased conversion of T effector cells to Treg cells [9].

Biomarkers such as PD-L1 expression, tumour-infiltrating lymphocyte (TIL), and tumour mutational burden (TMB) have also been evaluated recently, which promoted the predictive efficiency of immune therapy [10].

Nowadays studies has introduced the immune checkpoint inhibitor (ICI) into the combination strategies of HER2-targeted treatments, which activated T cells as well as enhanced Antibody Dependent Cellular Phagocytosis (ADCC) in vivo, and substantially improved response rate and median overall survival (OS) of HER2-positive treatment-naive patients [9,11].

As a typical feature of the S100 protein family, the aberrant expression of the calcium binding protein A9 (S100A9) of S100 is observed in multiple types of cancer tissues [12,13]. By forming heterodimer with S100A8 and binding with receptor for advanced glycation end products (RAGE) through mitogen-activated protein kinase (MAPK) pathway, intracellular S100A9 and its family

Table 1
Baseline characteristics of participants involved in this study.

Characteristic	No. (n = 667)	%
Age (years)		
Median (range)	47 (28–70)	–
≤50	356	53.33
>50	311	46.67
Menopause status		
premenopausal	269	40.28
postmenopausal	398	59.72
Pathological stage		
I	156	23.33
II	325	48.79
III	186	27.88
Histological grade		
1	212	31.82
2	277	41.52
3	178	26.66
Ki67 score (%)		
>20%	412	61.82
≤20%	255	38.18
LVSI[a] status		
positive	382	57.27
negative	285	42.73
pLN[b] number		
>3	236	35.45
≤3	431	64.55
Local therapy		
Mastectomy + ALND[c] + RT[d]	83	12.42
Mastectomy + ALND	234	35.15
Mastectomy + SLNB[e] + RT	72	10.61
Mastectomy + SLNB	198	29.70
BCS[f] + ALND + RT	42	6.36
BCS ++ SLNB + RT	38	5.76

[a] LVSI, Lymph-vascular space invasion.
[b] pLN, Pathological-diagnosed lymph node metastasis.
[c] ALND, Axillary lymph node dissection.
[d] RT, Radiation therapy.
[e] SLNB, Sentinel lymph node biopsy.
[f] BCS, Breast-conserving surgery.

members are widely involved in the process of energy metabolism and cellular response, whereas extracellular S100A8/S100A9 heterodimer contributes to the viability and migration of tumour cells in a concentration-dependent manner [14,15]. The expression and abundance of S100A9 in BRCA present some subtype specificities, which are associated with hormone receptor status [14]. Previous studies have also reported that overexpression of S100A9 could be associated with a poor survival outcome in HER2-positive settings [14,15]. Furthermore, the S100 protein family is also crucial to aerobic glycolysis [16] and lymphocyte recruitment [17]. Collectively, as a potential characteristic marker of HER2+ BRCA, S100A9 may play a key role in glycolysis-related immune suppression of TME, even affecting the therapeutic response and prognosis. To reveal the metabolism-related and immune-related effect of S100A9 in HER2+ BRCA, we explored S100A9 level in several distinct BRCA subtypes. Then, we evaluated the relationship between S100A9 intensity and glycolysis activity in HER2+ BRCA cases, as well as the signal pathway involved in this process. Furthermore, we assessed the proportion of different TIL subsets according to S100A9 level, thus describing the immune suppression in abundant cases of S100A9. Finally, we investigated the impact of S100A9 intensity on the survival of HER2+ BRCA.

2. Materials and methods

2.1. Study participants

Patients were pathologically diagnosed as HER2+ BRCA by core needle biopsy of breast lesions and clinically positive lymph nodes, which was defined as immunohistochemistry (IHC)-positive for HER2 3+ or by fluorescence in situ hybridisation (FISH) positive. A total of 667 cases were included in this study. Their characteristics were extracted from the database of the Breast Cancer Center of the Xiangya Hospital, Central South University (Table 1). All cases were enrolled between January 2016 and January 2019. Patients with inflammatory breast cancer, distant metastasis disease or bilateral breast tumors were excluded. All cases involved underwent radical surgery, such as breast preservation surgery and modified radical mastectomy. Adjuvant therapy was performed within 1 month after the surgery and consisted of taxane and carboplatin-based chemotherapy (intravenously on day 1 and every 21 days for 6 cycles) and trastuzumab (6 mg/kg; after a loading dose of 8 mg/kg, it was administered every 3 weeks for 1 year). Local advanced cases and breast-conserving cases received normative radiation therapy according to guidelines. Treatment details and pathological characteristics were collected from hospital medical records, including age, menopause status, pathological stage, histological grade, Ki-67 labelling index and invasion of lymph-vascular space (Table 1). Local or distant recurrence was regarded as the endpoint of follow-up. The study was carried out in accordance with the Declaration of Helsinki (as revised in 2013). The study was approved by the Ethics Committee of the Xiangya Hospital (approved number 202004189). Individual informed consent for this study was securely stored.

2.2. Reagents

Primary human antibodies for lactate dehydrogenase A (LDHA) (DF6280), phosphoglycerate kinase 1 (PGK1) (DF6722), enolase α (ENO1) (DF6191), β-catenin (AF6266) and c-Myc (AF0358) were purchased from Affinity Biosciences Ltd., Jiangsu, China. Primary human antibodies of S100A9 (bs-2697R), cluster of differentiation 3 receptor (CD3) (bs-0765R), cluster of differentiation 4 receptor (CD4) (bs-0647R), cluster of differentiation 8 receptor (CD8) (bs-4790R) and Forkhead/winged-helix transcription factor P3 (FOXP3) (bs-0269R) were obtained from BIOSS biosciences, Ltd., Beijing, China. Horseradish peroxidase (HRP)-conjugated secondary antibodies were also purchased from BIOSS (bs-0295G-HRP).

2.3. Cell culture and treatment

After considering the gene expression profile according to CCLE (https://sites.broadinstitute.org/ccle), metabolic activity in pilot experiment and use in previous studies (https://pubmed.ncbi.nlm.nih.gov), we finally chose SK-BR-3 (RRID: CVCL_0033) and BT474 (RRID: CVCL_0179). These two cell lines were cultured in 1640 medium containing 10% foetal bovine serum, 100 U/mL penicillin and 100 U/mL streptomycin. Cell culture was maintained at 37 °C in an atmosphere containing 5% CO_2 and saturated humidity in a constant temperature incubator. The culture medium was replaced every 2–3 days.

2.4. Small interference RNA transfection and reverse transcription quantitative polymerase chain reaction

Meanwhile, cells of S100A9 silenced group were transfected with the small interference RNA (siRNA) targeting S100A9 (NM002965.4, Sangon Biotech Co., Ltd. Shanghai, China), which was followed by culturing in Opti-MEM (Gibco, 31985-070) and Lipofectamine 3000 (Invitrogen, L3000-015). After incubation at 37 °C and 5% CO2 for 24 h, these S100A9 silenced cells were used to detect S100A9 expression by reverse transcription quantitative polymerase chain reaction (RT-qPCR). Total RNA was extracted following the instructions of the total RNA extraction kits (Solarbio Science&Technology Co., Ltd. Beijing, China). cDNA was collected

Table 2
Primer sequences used in RT-qPCR.

Gene	Forward primer	Reverse primer
S100A9	5′- GTGCGAAAAGATCTGCAAAA-3′	5′- TCAGCTGCTTGTCTGCATTT-3′
β-actin	5′- CCTGGGCATGGAGTCCTGTG-3′	5′- AGGGGCCGGACTCGTCATAC-3′

using reversed transcription kits (Yeasen Biotechnology Co., Ltd. Shanghai, China). RT-qPCR was performed using the Hieff® qPCR SYBR Green Master Mix. β-Actin was used as a control for normalisation. The primer sequences for S100A9 and β-actin are listed in Table 2. According to the triplicate identification of S100A9-Homo-88, S100A9-Homo-151 and S100A9-Homo-238 with a no-template control, S100A9-Homo-88 was validated as the most effective and was thus used in this study. Amplification was carried out at 95 °C for 5 min, followed by 40 cycles of 10 s at 95 °C, 20 s at 60 °C and 2 s at 72 °C.

2.5. Histopathology examination

The samples were embedded in an optimal cutting temperature compound (OCT) and cut into 6–8 μm thick slices using a frozen slicer. The slices were then fixed with 4% paraformaldehyde, dehydrated with anhydrous ethanol, mounted with neutral balsam and finally stained with haematoxylin and eosin (H&E). The slides were viewed twice by two experienced pathologists and the TIL labelling was blindly assessed.

Stromal TIL within the invasive lesions were evaluated according to the criteria recommended by the International TILs Working Group 2014, and was defined by the ratio of the area occupied by TILs to the total stromal area [18]. TILs beyond the tumour border or around the ductal carcinoma in situ (DCIS) were excluded. Areas with crush artifacts, necrosis and regressive hyalinisation were not included. The TIL level was assigned scores of 0–2 (0–10%, 11%–20% and >20%). Antibodies including CD3, CD4, CD8 and FOXP3 were used to distinguish TIL subsets.

2.6. Immunohistochemical staining

Relevant antibodies were used to evaluate the expressions of S100A9, LDHA, PGK1, ENO1, CD3, CD4, CD8 and FOXP3 in tumour tissues. The frozen sections were fixed in formaldehyde and dehydrated with anhydrous ethanol. Sections were placed in citrate buffer and incubated with 3% hydrogen peroxide to block endogenous peroxidase. The slices were then incubated with the above monoclonal antibodies (1:300 dilution) overnight at 4 °C after incubation with HRP-labelled secondary antibody for 50 min at room temperature. A 0.05% 3,3-diaminobenzidine tetrachloride (DAB) solution was added until the brownish reaction was visualised, and finally, haematoxylin was used for counter staining. The OLYMPUS DP26 light microscope was used to observe the slides. The staining results were analyzed using Image J 1.8.0.112 software. Tumour cells stained with brown-yellow colouring were considered regions of interest (ROI). The proportion of ROI was assigned as levels 1–4 (10%, 11%–25%, 26%–75% and ≥76%, respectively), and the intensity of ROI was also assigned as grades 1–4 (no staining = 0, weak = 1, moderate = 2 and strong = 3). Finally, the staining results were simplified as multiplication of proportion and intensity that ranged from scores 0 to 12, and cases with scores greater than 4 were considered positive [19].

2.7. Western blot analysis

Relevant antibodies were used to evaluate the expressions of S100A9, LDHA, PGK1, ENO1, β-catenin and c-Myc in cell lines. The cells were lysed on ice for 20 min and centrifuged at 12000 RPM at 4 °C for 20 min. The supernatant was collected, and the lysate protein was quantified using bicinchoninic acid (BCA) assay. Then, 10% sodium dodecyl sulphate-polyacrylamide gel electrophoresis (SDS-PAGE) was used to separate proteins. PVDF membrane blotting was processed at 4 °C (ice bath) and 200 mA for 90 min (0.45 μm). Then, blocking with 5% TBST was performed for 2 h, and membranes were incubated with primary antibodies (1:1000 dilution) at 4 °C overnight. The membranes were then incubated with HRP-tagged secondary antibody for 2 h at room temperature and exposed to enhanced chemoluminescence (Beyotime, P0018S-2) for 20 min. The automatic chemiluminescence image analysis system (Tanon, 5200) was used for exposure. The exposure results were analyzed with Image J 1.8.0.112 software to calculate the optical density (OD) and the grey value of the individual blotting.

2.8. Immunofluorescence assay

Relevant antibodies were used to evaluate the expressions of S100A9, LDHA, PGK1, ENO1, β-catenin and c-Myc in tumour cells. The cells were centrifuged at 2800 RPM at 4 °C for 5 min, fixed with 4% paraformaldehyde and permeabilised with 0.1% Triton X-100 (BIOSS, P0096) at room temperature for 20 min. The cells were then washed with PBS (Solarbio, P1022) and blocked with 3% bovine serum albumin (BSA) (BIOSS, bs-0292P) at room temperature for 30 min. Then, incubation with primary antibodies (1:300 dilution) was performed at 4 °C overnight and HRP-tagged secondary antibody (1:500 dilution) for 50 min at room temperature. DAPI (BIOSS, C02-04002) was used for nucleus staining. Anti-fade mounting medium (Solarbio, S2110) was used for mounting.

2.9. Detection of glucose consumption and lactate production

When glucose consumption was measured, normal control and S100A9 silencing cells were first incubated in glucose-free medium for 12 h (glucose starvation), after culture in medium was added to 2-deoxyglucose (2-DG) and incubated for 20 min at 37 °C. 2-DG was taken up by cells and metabolised to 2-DG-6-phosphate (2-DG6P), which accumulated within cells and finally oxidised. Then, 2-DG uptake was detected following the manufacturer's introductions (glucose uptake assay kit, BioVision/Abcam, ab136955).

When measuring lactate production, normal control and S100A9 silencing cells were successively cultured in routine and phenol-free medium. Then, cell culture supernatants were collected and used to measure lactate concentration by detecting absorbance at 450

nm following the manufacturer's introductions (Lactate Assay Kit, BioVision/Abcam, ab83429).

2.10. Detection of the extracellular acidification rate

Seahorse XFe 96 Extracellular Flux Analyzer (Agilent Technologies Inc., California, USA) was used to assess the extracellular acidification rate (ECAR) (mpH/min). Cells were seeded in a Seahorse XF 96 cell culture microplate (1×10^4 cells/well) the day before the experiment. The sensor cartridge was hydrated with Seahorse XF calibration solution and preheated at 37 °C overnight. Reagents in the glycolysis stress test kit (glucose, oligomycin and 2-DG) were configured according to the instructions and sequentially injected at the indicated points. The results were output via Seahorse wave software.

2.11. Bioinformatics analyses

Gene enrichment analysis was performed using gene set enrichment analysis (GSEA) version 4.1.0 for Windows (Broad Institute, Cambridge, Massachusetts, USA, RRID: SCR_003199), whose significance was evaluated using the normalised enrichment score (NES) and the false discovery rate (FDR). Differential expression-interested genes were graphically depicted by several online bioinformatics tools, including GEPIA (http://gepia2.cancer-pku.cn/) and UALCAN (http://ualcan.path.uab.edu/). The lymphocyte recruitment effect of S100A9 was assessed using TIMER 2.0 (http://timer.cistrome.org/). The above analyses were taken from the Cancer Genome Atlas (TCGA) database.

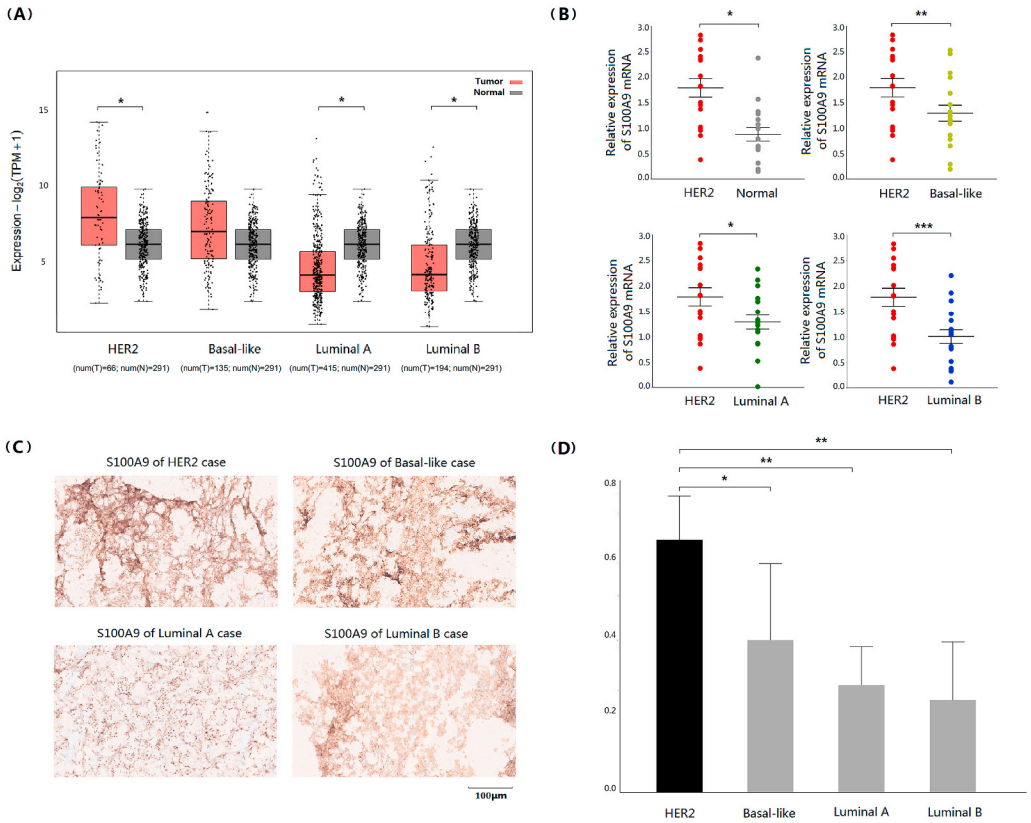

Fig. 1. (A) Upregulation of S100A9 in BRCA tissues (compared with corresponding adjacent tissues) was significant in the HER2+ subgroup (*, $p < 0.05$). (B) RT-qPCR results of tumour tissues from distinct BRCA subgroups (90 cases were involved, 18 for each subgroup) confirmed the abundant S100A9 intensity in HER2+ BRCA cases (*, $p < 0.05$; **, $p < 0.01$; ***, $p < 0.001$). Median expression level of HER2, Luminal A, Luminal B, basal like, and normal cases were 1.7830, 1.2867, 1.0033, 0.8769, and 1.2829, respectively. (C) IHC staining results of tumour tissues from distinct BRCA subgroups (40 cases were involved, 10 for each subgroup. Typical representative was chosen for presentation. Scale bar = 100 μm) confirmed the abundant S100A9 intensity in HER2+ BRCA cases (scale bar = 100 μm). (D) Western blotting results of tumour tissues from distinct BRCA subgroups (20 cases were involved, 5 for each subgroup) confirmed the higher S100A9 intensity in HER2+ BRCA cases (*, $p < 0.05$; **, $p < 0.01$, Non-HER2 means the sum of Luminal A, Luminal B, and Basal-like cases). S100A9: S100 calcium-binding protein A9. BRCA: Breast cancer. HER2: Human epidermal growth factor receptor 2. RT-qPCR: real-time quantitative polymerase chain reaction. IHC: Immunohistochemical staining.

2.12. Statistical analyses

Statistical analyses, such as the *t*-test and receiver operating characteristic (ROC) curve, were conducted using Graphpad Prism version 8.0 for Windows (GraphPad Software Inc., San Diego, California, USA, RRID: SCR_002798). Kaplan-Meier survival curves were derived from the KM plotter database (http://kmplot.com). The Cox proportional hazards model was used to analyse the prognostic value of the variables. The results were expressed as hazard ratios (HR) and 95% confidence intervals (CI). Cox proportional hazards analysis was performed using SPSS version 25.0 (SPSS Inc., Chicago, Illinois, USA, RRID: SCR_002865). The cumulative incidence

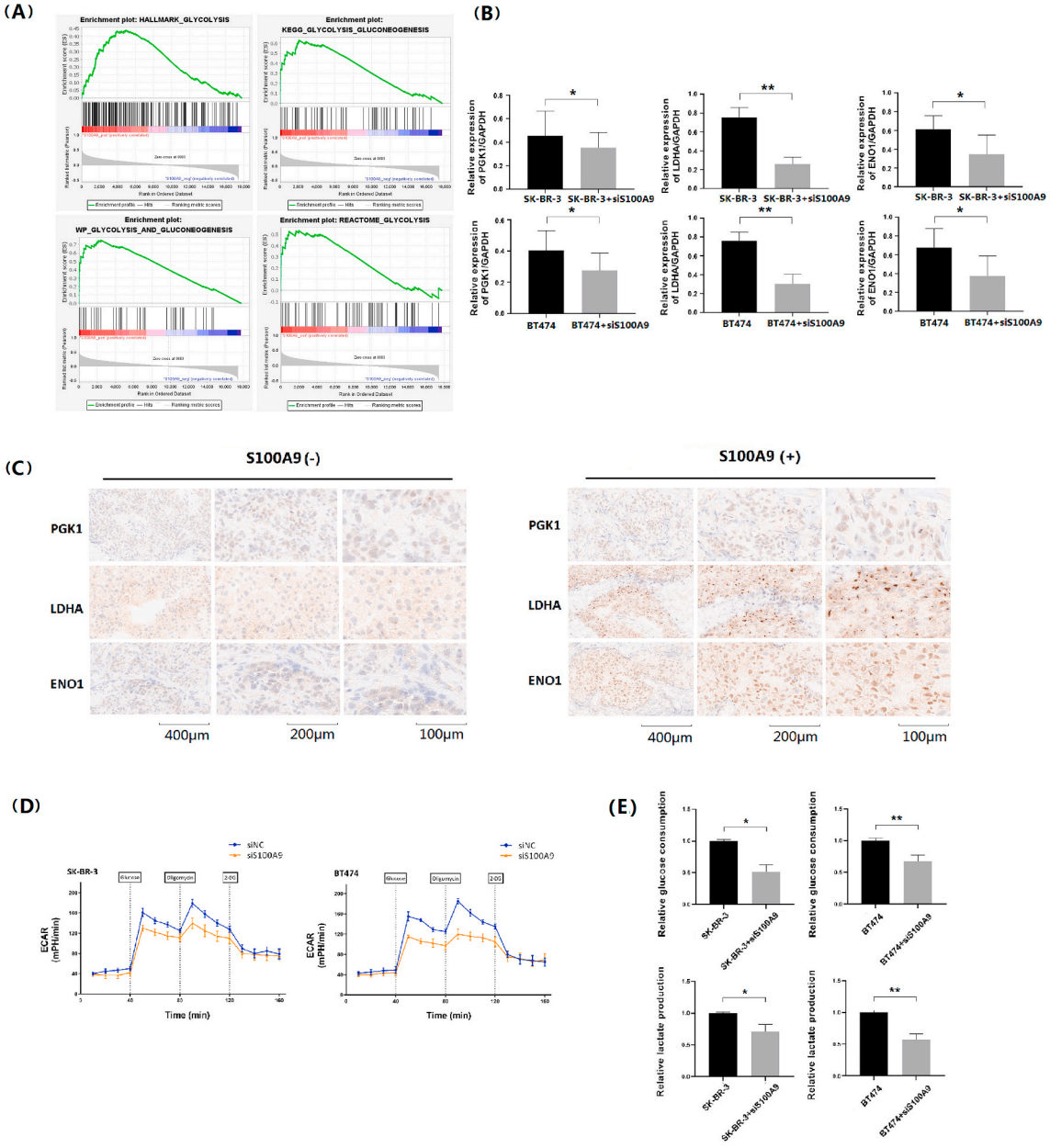

Fig. 2. (A) Enrichment of glycolysis-related genes was significant in S100A9 positive BRCA cases (NES > 1, FDR q-value < 0.001). (B) S100A9 silencing impaired the expression of PGK1, LDHA, and ENO1 in both SK-BR-3 and BT474 cell lines. (C) IHC staining results of HER2+ BRCA tissues confirmed the upregulation of PGK1, LDHA, and ENO1 in S100A9 abundant cases (Scale bar = 100 μm, 200 μm, and 400 μm). (D) ECAR level significantly declined when S100A9 was absent from the SK-BR-3 and BT474 cell lines. (E) lactate production and glucose consumption level significantly declined when S100A9 was absent from the SK-BR-3 and BT474 cell lines. PGK1: Phosphoglycerate kinase 1. LDHA: Lactate dehydrogenase A. ENO1: Enolase α. ECAR: Extracellular acidification rate. S100A9: S100 calcium-binding protein A9. BRCA: Breast cancer. HER2: Human epidermal growth factor receptor 2. NES: Normalised enrichment score. FDR: False discovery rate. IHC:Immunohistochemical staining.

model was used to assess the risk of relapse that increased with increasing intensity of S100A9. Heterogeneity of adjuvant immunotherapy effects was evaluated by the permutation inference distribution. Cumulative incidence analysis and permutation inference distribution were carried out using the R version 4.0.4 software package (R Foundation for Statistical Computing, Vienna, Austria; RRID: SCR_001905). All statistical tests were two-sided, and p-values less than 0.05 were considered statistically significant.

3. Results

3.1. Aberrant expression of S100A9 in HER2+ BRCA cases (TCGA BRCA database)

Based on the TCGA BRCA database, we conducted a comprehensive evaluation of the relationship between S100A9 and HER2. S100A9 level of tumour tissues was significantly higher than that of normal tissues in the HER2 subgroup, whereas the situation was completely opposite in Luminal A/B cases. No significant difference was observed between tumour and normal tissues in basal-like cases (Fig. 1A).

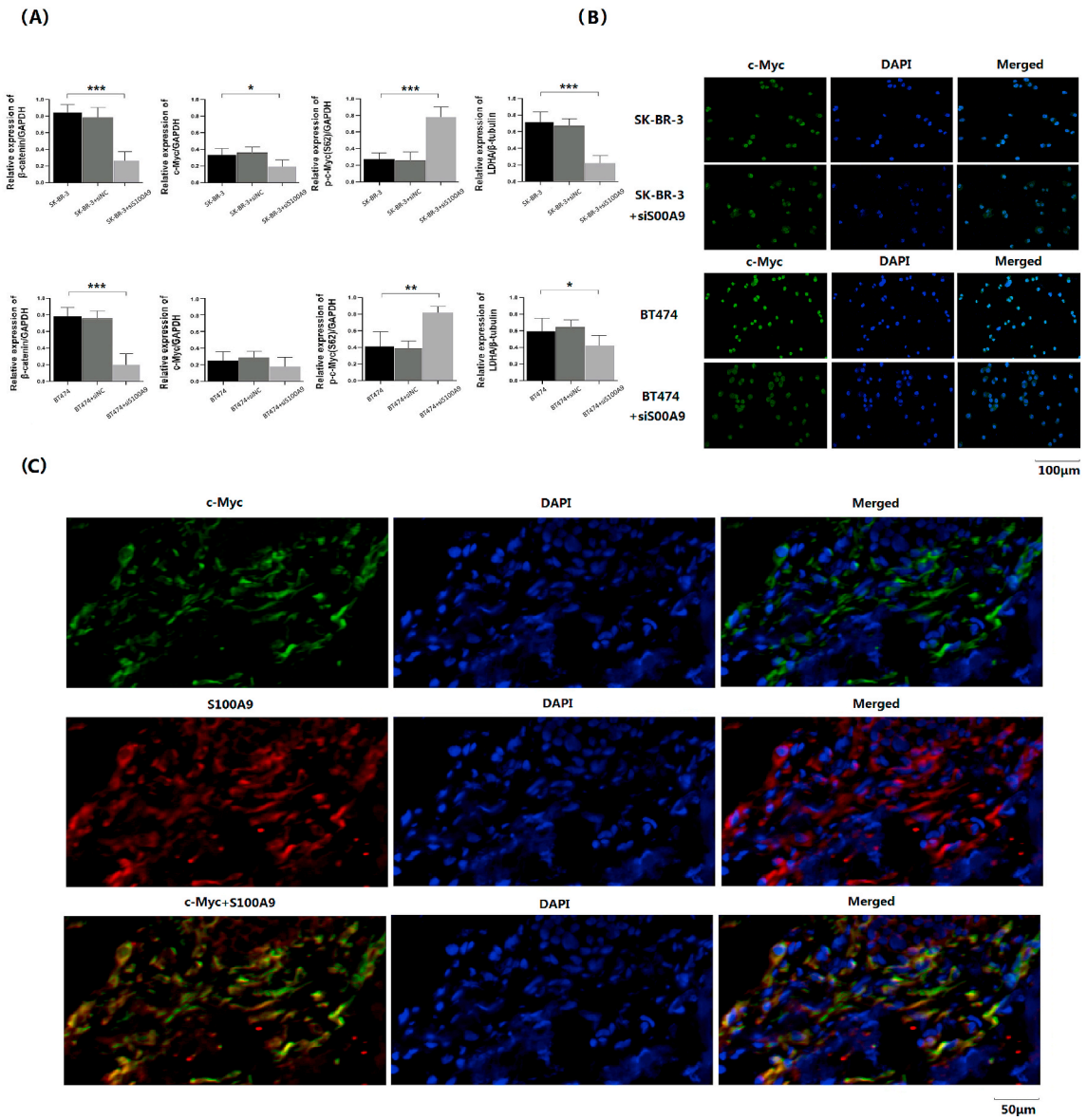

Fig. 3. (A) S100A9 silencing induced down-regulation of β-catenin and c-Myc, and subsequently prompted the phosphorylation of c-Myc in both SK-BR-3 and BT474 cell lines. (B) Immunofluorescence staining results confirmed that nuclear localisation of c-Myc decreased in S100A9 silencing cell lines (Scale bar = 100 μm). (C) Double-label immunofluorescence staining results of HER2+ BRCA tissues confirmed the co-expression of S100A9 and c-Myc (Scale bar = 50 μm). S100A9: S100 calcium-binding protein A9. BRCA: Breast cancer. HER2: Human epidermal growth factor receptor 2.

As shown in the Supplemental Fig. 1A, type-specific comparison via ROC curves between subgroups showed outstanding sensitivity and specificity of S100A9 in HER2+ BRCA. Furthermore, genes that contributed to the upregulation of HER2, such as GRB7, IGF2R and ITGB6, tended to be enriched in abundant cases of S100A9, according to the GSEA results (NES 1.769, FDR q-value<0.001) (Supplemental Fig. 1B). The volcano plot also visually revealed a positive presentation in cases of HER2+ BRCA (Log_2 fold change 1.031, adjusted p-value 9.167E-05) (Supplemental Fig. 1C), whereas Pearson's analysis supported a transcriptional correlation between S100A9 and HER2 (Supplemental Fig. 1D).

3.2. Aberrant expression of S100A9 in HER2+ BRCA tumour tissues

To confirm the higher expression of S100A9 in cases of HER2+ BRCA, we performed RT-qPCR (Fig. 1B), IHC (Fig. 1C) and WB assay (Fig. 1D) using tissues with distinct BRCA subtypes. As shown in Fig. 1B, significantly higher expression of S100A9 was detected at mRNA level in HER2+ cases than in normal cases (1.7830 vs. 1.2829, fold change 1.39, $p = 0.033$), basal-like cases (1.7830 vs. 1.0033, fold change 1.78, $p = 0.001$), luminal A cases (1.7830 vs. 1.2867, fold change 1.39, $p = 0.043$) and luminal B cases (1.7830 vs. 0.8769, fold change 2.03, $p < 0.001$). According to the chromatic aberration, IHC staining assay showed obvious overexpression of S100A9 at the protein level in HER2+ cases than in other cases (Fig. 1C). According to the optical density value of gels, western blotting assay

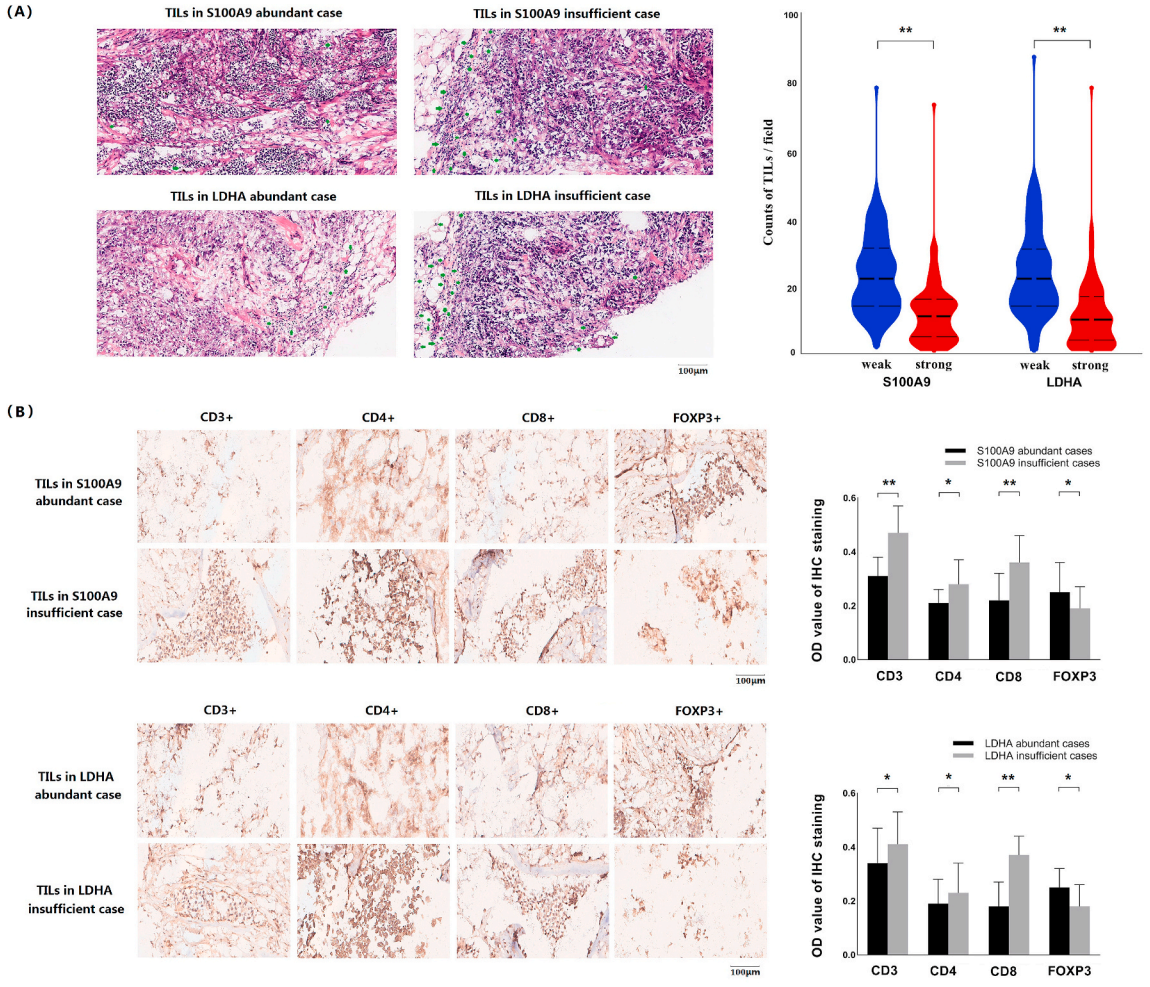

Fig. 4. (A) H&E staining results of HER2+ BRCA tissues confirmed the negative relation between TILs infiltration and S100A9/LDHA intensity (10 cases for each subgroup. Typical representative was chosen for presentation. Scale bar = 100 μm; **, $p < 0.01$. TILs were pointed out by green arrows). (B) IHC staining results of HER2+ BRCA tissues revealed that CD3+/CD4+/CD8+ TILs were enriched in the S100A9 sparse cases, while FOXP3+ TILs mostly infiltrated in S100A9 sufficient cases (10 cases for each subgroup. Typical representative was chosen for presentation. Scale bar = 100 μm; *, $p < 0.05$; **, $p < 0.01$). S100A9: S100 calcium-binding protein A9. BRCA: Breast cancer. HER2: Human epidermal growth factor receptor 2. PGK1: Phosphoglycerate kinase 1. LDHA: Lactate dehydrogenase A. ENO1: Enolase α. TILs: Tumour infiltrating lymphocytes. H&E: Haematoxylin and eosin. IHC: Immunohistochemistry. CD3: Cluster of differentiation 3 receptor. CD4: Cluster of differentiation 4 receptor. CD8: Cluster of differentiation 8 receptor. FOXP3, Forkhead/winged-helix transcription factor P3. (For interpretation of the references to colour in this figure legend, the reader is referred to the Web version of this article.)

showed higher level of S100A9 in HER2+ cases than in basal-like cases (0.64 ± 0.13 vs. 0.42 ± 0.22, p = 0.029), luminal A cases (0.64 ± 0.13 vs. 0.33 ± 0.18, p = 0.008) and luminal B cases (0.64 ± 0.13 vs. 0.25 ± 0.17, p = 0.005) (Fig. 1D). These findings were all consistent with the results of bioinformatics analysis described above.

3.3. S100A9-modulated glycolysis activity via c-Myc relevant pathway in HER2+ BRCA cell lines and tumour tissues

Bioinformatics analysis based on the TCGA database revealed the significant enrichment of glycolysis-related pathways (Fig. 2A). To investigate the role of S100A9 in regulating the expression of glycolytic enzymes, normal control and S100A9-silenced cells were subjected to a Western blot assay using anti-PGK1, anti-LDHA and anti-ENO1 antibodies. According to the optical density value of gels, a significant decline in PGK1 (p = 0.037 for SK-BR-3, p = 0.040 for BT474), LDHA (p = 0.005 for SK-BR-3, p = 0.007 for BT474) and ENO1 (p = 0.028 for SK-BR-3, p = 0.032 for BT474) expressions was detected in S100A9 silenced cell lines (Fig. 2B). Furthermore, we compared the expressions of PGK1, LDHA and ENO1 in tissues of HER2+ BRCA according to the intensity of S100A9 and verified the upregulation of these enzymes in cases with a higher level of S100A9, which was consistent with the *in vitro* results above (Fig. 2C).

As shown in the Supplemental Fig. 2, bioinformatics analysis based on the TCGA database revealed the upregulation of crucial enzymes, such as PKM2, ENO1, TPI, PGK1 and LDHA, in S100A9-positive BRCA cases.

3.4. S100A9 modulated glycolysis activity in HER2+ BRCA cell lines

Besides the differential expression phenotype at the protein level, functional experiments were also performed *in vitro* to evaluate the influence of S100A9 on lactate production and glucose consumption. A significant decline in ECAR along with S100A9 deficiency was observed in both the SK-BR-3 and BT474 cell lines, suggesting the obvious effect of S100A9 on the accumulation of lactic acid (Fig. 2D). As shown in Fig. 2E, the concentration of lactate in cultured medium (p = 0.019 for SK-BR-3, p = 0.004 for BT474) and glucose uptake of tumour cells (p = 0.625 for SK-BR-3, p = 0.007 for BT474) were significantly impaired by S100A9 silencing.

3.5. S100A9 induced activity of c-Myc relevant pathway in HER2+ BRCA cell lines and tumour tissues

As a crucial transcription factor that affects the metabolic activity of tumour cells, c-Myc is involved in the regulation of many glycolysis-related genes. Given the obvious effect of S100A9 on glycolysis activity, we assumed that there may be a connection between S100A9 and c-Myc. To verify our hypothesis, we first investigated the role of S100A9 in c-Myc-targeted pathways. We evaluated

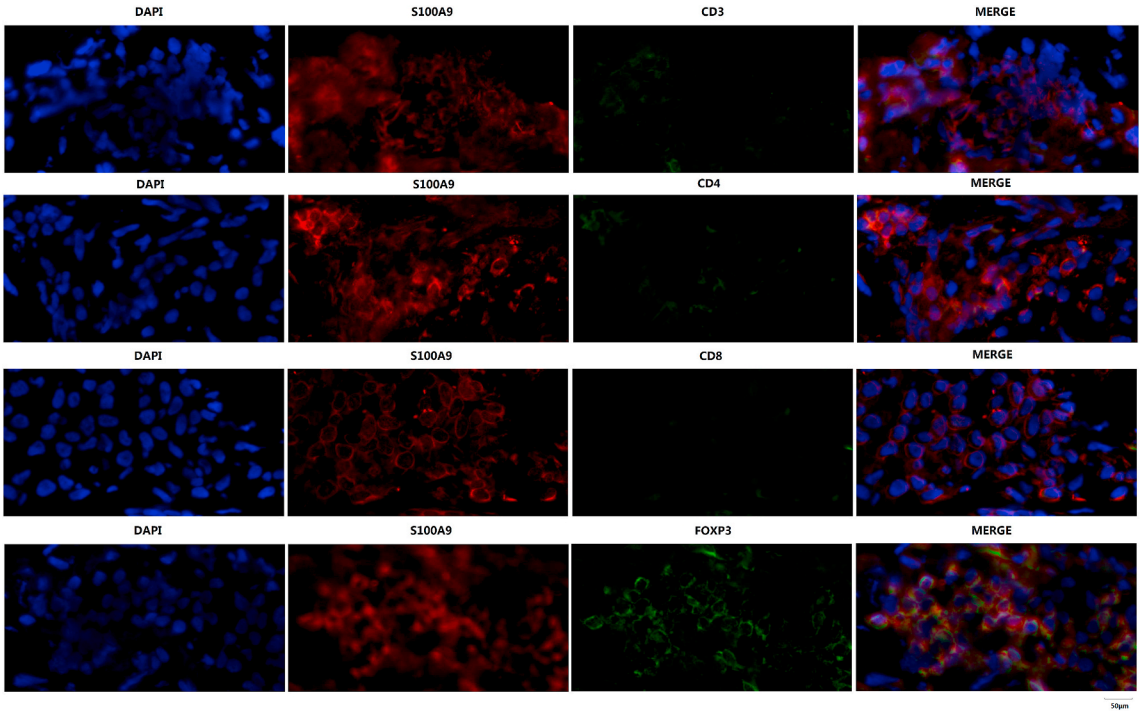

Fig. 5. Double-label immunofluorescence staining results of HER2+ BRCA tissues confirmed that CD3+/CD4+/CD8+ TILs enriched in the S100A9 sparse cases, while FOXP3+ TILs mostly infiltrated in S100A9 sufficient cases (10 cases were involved). Typical representative was chosen for presentation (scalebar = 50 μm). S100A9: S100 calcium-binding protein A9. BRCA: Breast cancer. HER2: Human epidermal growth factor receptor 2. CD3: Cluster of differentiation 3 receptor. CD4: Cluster of differentiation 4 receptor. CD8: Cluster of differentiation 8 receptor. FOXP3: Forkhead/winged-helix transcription factor P3. TILs: Tumour infiltrating lymphocytes.

the protein levels of c-Myc and its downstream regulators in normal control cell lines and in those with S100A9 silencing. As shown in Fig. 3A, the absence of S100A9 greatly hindered the expression of β-catenin ($p < 0.001$ for both SK-BR-3 and BT474), which targeted c-Myc as a transcription activator. Subsequently, notable upregulation of phosphorylated c-Myc ($p < 0.001$ for SK-BR-3, $p = 0.015$ for BT474) and the decline of c-Myc ($p = 0.042$ for SK-BR-3, $p = 0.156$ for BT474) were observed. Interestingly, a decrease in LDHA ($p < 0.001$ for SK-BR-3, $p = 0.034$ for BT474) appeared along with the S100A9-induced inhibition of the β-catenin/c-Myc pathway, which was consistent with the relationship between S100A9 and LDHA shown in Fig. 2. As indicated by Fig. 3B, we observed that nuclear localisation of c-Myc was sparse in S100A9 silenced cells with the corresponding elevated intensity of c-Myc in the cytoplasm. Furthermore, we also investigated the cytoplasmic co-expression of S100A9 and c-Myc in HER2+ BRCA tissues and revealed that the enrichment of c-Myc was consistent with the abundant intensity of S100A9, which corroborated the above *in vitro* results (Fig. 3C).

As shown in the Supplemental Fig. 3A, we observed a significant enrichment of c-Myc-targeted genes in S100A9-positive cases according to the results of GSEA. The relationship between S100A9 and c-Myc was apparent at the transcription level (Supplemental Fig. 3B), and the expression of S100A9 was up-regulated in c-Myc amplified metastatic BRCA cases (Supplemental Fig. 3C).

3.6. S100A9-induced glycolytic activation and TILs deficiency in HER2+ BRCA tissues

Next, we assessed the immune cell infiltration according to the intensity of S100A9 and LDHA in HER2+ BRCA specimens. As indicated in Fig. 4A, the total counts of TILs were obviously higher in cases with a higher expression of S100A9 than in cases with lower S100A9 levels ($p = 0.003$), whereas the TIL amount of LDHA-abundant cases was much greater than the LDHA-poor cases ($p = 0.006$). Furthermore, we explored the distribution of TIL subsets according to the S100A9 and LDHA levels. As shown in Fig. 4B, CD4+/CD8+ T cells tended to infiltrate the stroma of S100A9-poor BRCA slices ($p = 0.028$, $p = 0.004$, respectively), whereas FOXP3+ T cell infiltration was elevated in S100A9-enriched cases ($p = 0.047$). Similar trends were also detected based on the intensity of LDHA ($p = 0.017$ for $CD4^+$ subset, $p = 0.006$ for $CD8^+$ subset and $p = 0.029$ for FOXP3+ subset).

As shown in Supplemental Fig. 4A, genes involved in suppression of leukocyte function tended to be enriched in S100A9-positive BRCA cases, which might alter leukocyte-mediated immunity. According to the TCGA database, the expression intensities of PGK1, LDHA and ENO1 were negatively correlated with the level of infiltration of CD4+/CD8+ T cells (Supplemental Fig. 4B).

We also verified the heterogeneous distribution of the TIL subsets according to S100A9 and LDHA levels via double-label immunofluorescence assay, which was proved to be consistent with the IHC staining results. As shown in Fig. 5, CD3+/CD4+/CD8+ T cells were generally rare in S100A9 dominant cases, whereas FOXP3+ T cells tended to infiltrate cases with a higher S100A9

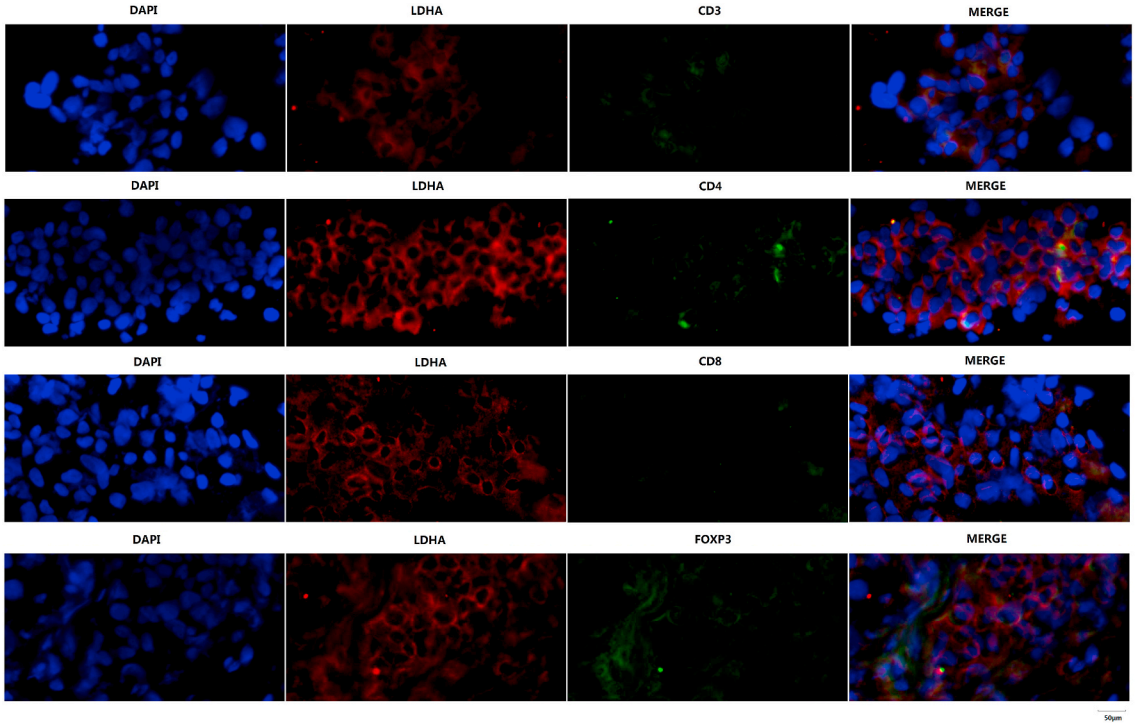

Fig. 6. Double-label immunofluorescence staining results of HER2+ BRCA tissues revealed that CD3+/CD4+/CD8+ TILs tended to infiltrate LDHA-poor cases, whereas FOXP3+ T cell infiltration was elevated in LDHA-abundant cases (10 cases were involved). Typical representative was chosen for presentation (scale bar = 50 μm). LDHA: Lactate dehydrogenase A. BRCA: Breast cancer. HER2: Human epidermal growth factor receptor 2. CD3: Cluster of differentiation 3 receptor. CD4: Cluster of differentiation 4 receptor. CD8: Cluster of differentiation 8 receptor. FOXP3: Forkhead/winged-helix transcription factor P3. TILs: Tumour infiltrating lymphocytes.

expression. Similar distribution of TIL subsets was also detected based on the intensity of LDHA (Fig. 6).

3.7. Poor immunotherapeutic efficacy and impairing cumulative survival in S100A9 abundant cases

Based on the survival analysis using the KM plotter database, we determined the effects of S100A9 intensity on the prognosis of different subgroups of BRCA. In both StGallen and PAM50 classified systems, the prognostic value of HER2+ BRCA was significantly impaired by higher S100A9 expression, which was distinct from other subgroups (Fig. 7). As shown in Fig. 8A, the prognostic

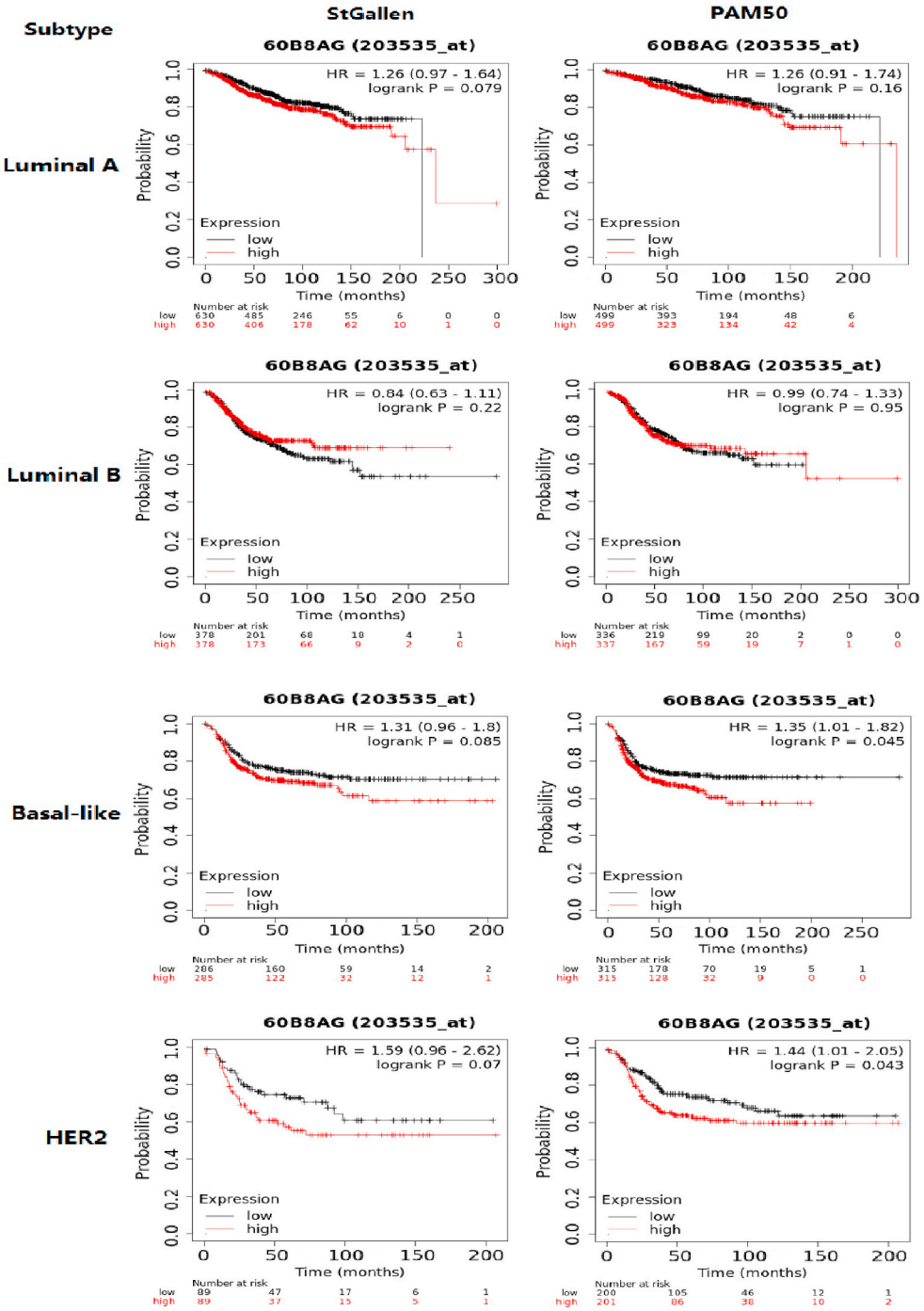

Fig. 7. Upregulation of S100A9 was mostly associated with poor survival of HER2+ BRCA cases according to both StGallen (p = 0.07) and PAM50 classified systems (p = 0.045). S100A9: S100 calcium-binding protein A9. HER2: Human epidermal growth factor receptor 2. HR: hazard ratio.

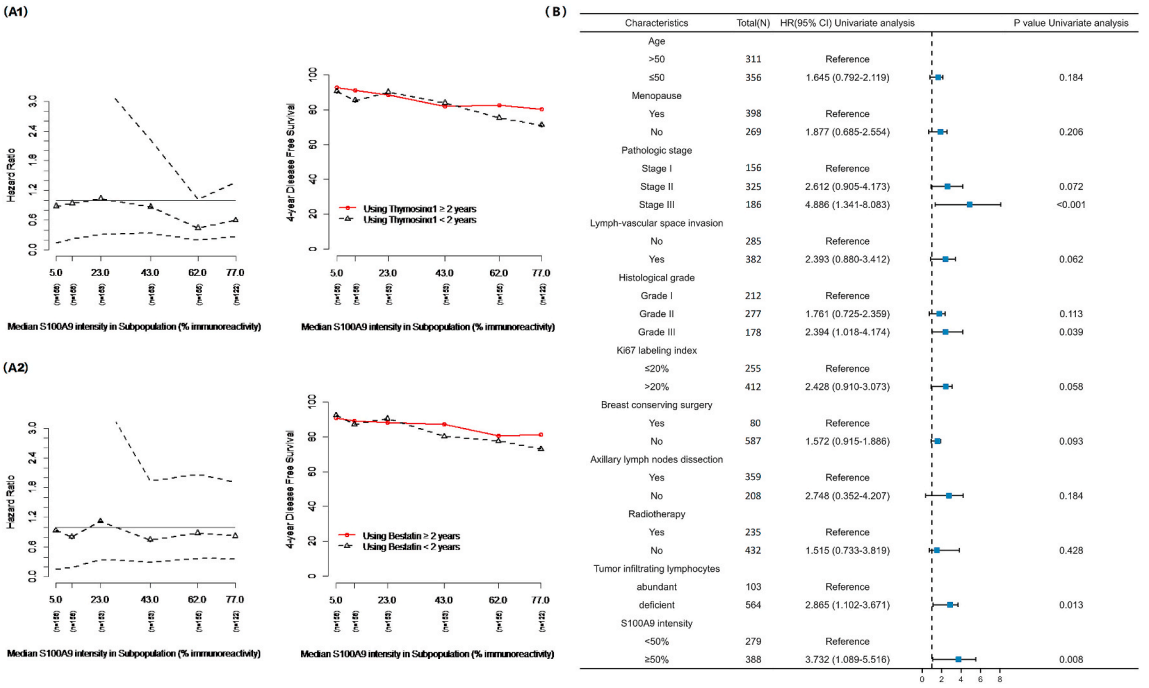

Fig. 8. (A) Recurrent risk increased along with the elevated intensity of S100A9. Long-term using of thymosin-α1 or bestatin (more than 2 years) improved survival, especially in S100A9 abundant sub-populations. (B) Advanced pathological stage, poor histological grade, absence of TILs, and upregulation of S100A9 mostly affected the long-term survival of HER2+ BRCA patients. Cox proportional hazards model, cumulative incidence model, and permutation inference distribution model were employed in survival analysis. S100A9: S100 calcium-binding protein A9. BRCA: Breast cancer. HER2: Human epidermal growth factor receptor 2. TILs: Tumour infiltrating lymphocytes.

improvement was obvious with the long-term (more than 2 years) treatment of thymosin-α1 or bestatin, indicating the importance of immune regulation therapy for HER2+ BRCA. In view of the decreased HR value combined with the higher expression of S100A9, we also observed that the therapeutic efficacy of immune regulation agents was more remarkable in S100A9 abundant sub-populations. In addition to well-known risk factors, such as higher pathological stage and lymph nodes metastasis, TIL deficiency and elevated S100A9 intensity also affected long-term survival of cases of HER2+ BRCA (Fig. 8B), which was consistent with the survival analysis based on the KM plotter database.

4. Discussion

4. Activation of S100A9/β-catenin/c-Myc axis: a new hallmark of HER2+ BRCA

Differential expression of S100A9 was higher in breast cancer and normal tissues, whereas its overexpression in tumour tissues was a predictive marker of disease progression [20]. The amplification of S100A9 was usually associated with a poor differentiation, such as in invasive breast duct carcinoma [12]. In particular, S100A9 was more highly expressed in HER2+ BRCA cases, which was correlated with negative hormone receptor status, vessel invasion, lymph node metastases and elevated Ki67expression [15]. Based on the online dataset Gene Expression Omnibus, Zhang et al. determined that the high mRNA level of S100A9 was directly related to worse survival of BRCA patients [21]. In this study, the overexpression of S100A9 was presented as an obvious hallmark of HER2+ BRCA tissues, which was consistent with the results of the bioinformatics analysis based on the TCGA database. Taking into account the significant expression of S100A9 in HER2+ cases at both the mRNA and protein level, higher S100A9 expression is a novel feature that distinguishes HER2+ cases from other BRCA subsets.

As a danger-associated molecular patterns (DAMPs), S100A9 exerts its biological role via cell surface receptors, such as Toll-like receptor 4 (TLR4) and the receptor for advanced glycation end products (RAGE), which drive the cross-regulation among the Wnt/β-catenin, MAPK and NK-κB signalling cascades and even triggered cellular responses [22–24]. Emerging evidence demonstrates that the oncogene c-Myc plays a vital role in metabolic reprogramming, which contributes to the activation of transcription regulators that participate in glycolysis [25]. Besides modulating LDHA and other glycolytic enzymes, the deregulated expression of c-Myc interferes with the enhancer sequences to hasten the amplification of these genes, providing excessive energy for tumour cell proliferation [26,27]. He et al. [28] observed that aberrant upregulation of S100A9 significantly induced the accumulation of β-catenin, whereas the knockdown of S100A9 caused a notable decrease of β-catenin, following the corresponding changes in c-Myc transcription. Basiorka et al. [29] and Duan et al. [30] also demonstrated that treatment with recombinant S100A9 led to β-catenin activation both in the

nucleus and cytoplasm and activated the β-catenin pathway to ultimately promote the transcription of its targeted gene, such as c-Myc. In this study, we verified the indispensable role of S100A9 in the glycolysis process. In addition to the down-regulation of LDHA and other key enzymes, *in vitro* silencing of S100A9 also altered lactate production and glucose uptake of tumour cells, which eventually caused a decrease in the ECAR. Furthermore, we detected a down-regulation of β-catenin/c-Myc and a subsequent upregulation of phosphorylated c-Myc in the absence of S100A9, which coincided with the decrease in LDHA expression in cell lines. We also confirmed the co-expression of S100A9 and c-Myc in HER2+ tissues. These findings suggested that S100A9 is involved in the activation of the β-catenin/c-Myc pathway; the latter was proven to be crucial in the glycolysis process.

4.2. The accumulation of glycolytic lactate altered TIL recruitment in HER2+ BRCA

A marked upregulation of glycolysis activity was observed in BRCA cells resistant to Lapatinib, which was manifested as an extensive phosphorylation of LDHA, ENO1 and other crucial enzymes [31]. Specifically, a selective inhibitor, such as saracatinib, reduced the translation of c-Myc, thus decreasing the expression of the above enzymes and interfering with glucose uptake [32]. Similarly, enhanced reprogramming of glycolysis could facilitate the resistance to targeted agents in HER2+ BRCA cases.

TILs played vital roles in the prognosis and therapeutic response of cancers [33]. Much like tumour cells, TILs also derive nutrients from TME. However, the correlation between glycolysis patterns and tumour immune efficacy has not been well investigated. Recent studies demonstrated that metabolic reprogramming played a role in immune escape of malignant cells, as highly glycolytic cancer cells competed with TILs for nutrition within the TME and exhausted glucose, thus affecting the function of TILs and altering the immune response mediated by T cells [34,35]. Furthermore, $CD8^+$ T cells rarely infiltrated metabolically vigorous lesions [36]. As a part of the metabolism-related oncogenic signalling pathway, the activation of c-Myc could increase tumour cell glycolysis [37]. Upregulation of c-Myc obviously inhibited oxidative phosphorylation accompanied by excessive expression of LDHA after the accumulation of lactate in the TME [38–40]. Lactic acid, a vital metabolite of rapid tumour cell proliferation, promotes the formation of immune escape and the activation of tumourigenic signalling [41]. Increased lactic acid level contributes to the dysfunction of cytotoxic T cells by inhibiting lymphocyte proliferation and cytokine production [9]. Tina et al. [42] reported that glycolytically dominant tumour cells caused an elevated level of lactic acid in immunosuppressive TME, whereas the use of the LDHA inhibitor rebuilt the antitumour activity of infiltrating cytotoxic lymphocytes. Brand et al. [9] also demonstrated a positive relationship between elevated LDHA intensity, elevated lactic acid level and the lack of cytotoxic T cell infiltration, whereas targeted inhibition of LDHA in cancer cells restored infiltration and function of effective $CD8^+$ T cells, which accounted for increased number and improved activation of $CD8^+$ T cells in the $LDHA^{low}$ phenotype. Furthermore, bioinformatics enrichment analysis revealed a negative relationship between glycolysis activity and CD4+/CD8+ TIL recruitment, because the lactic acid-enriched intercellular substance was insufficient for the activation and proliferation of cytotoxic T cells [43]. Therefore, an elevated intensity of LDHA was considered a predictive marker of poor survival [44]. In this study, we detected poor antitumour lymphocyte infiltration in S100A9 dominant cases, as well as abundant cases of LDHA. As the typical subsets of antitumour lymphocytes, $CD4^+$ T and $CD8^+$ T cells had low levels of S100A9 and LDHA. Conversely, FOXP3+ T cells were enriched in the corresponding cases; their appearance was harmful to the immune antitumour response. Given the immunosuppressive effect of LDHA demonstrated in the previous studies, we hypothesised that S100A9 overexpression impaired the antitumour immune activity by increasing the glycolysis process, which could explain the coexistence of LDHA overexpression and cytotoxic TIL deficiency in S100A9 dominant tumour tissues.

4.3. Abundant S100A9 induced immunosuppression via encouraging tumoural glycolysis

Imaoka et al. found that the upregulation of the S100A9 level supported tumour invasion via inflammatory cells in radiation-induced breast cancer [45]. S100A9-derived myeloid suppressor cells (MDSC) were explored to recruit them, which then exerted an immunosuppressive effect by inhibiting dendritic cell differentiation [17]. As the most selective antibody for S100A9, Ab45 significantly reduced the incidence of metastasis by inhibiting S100A9-induced chemotaxis [46]. The clinical trial also proved that an inhibitor of S100A9, such as tasquinimod, could improve progression-free survival by modulating the proportions of immune cells in the TME [47,48]. Therefore, S100A9 might play a crucial role in the impairment of the immune response to cancers, and treatment of its immune suppression would contribute to tumour remission and progress improvement. Based on multi-database analysis and our own follow-up, we observed the unsatisfactory survival of advanced cases of S100A9, especially in HER2+ subgroups, thereby suggesting the potential effect of S100A9 as a prognostic predictor. In addition to well-known risk factors, such as a higher pathological stage and lymph node metastases, TIL deficiency also affected the long-term survival of participants in this study, suggesting the need for immune therapy in HER2+ patients. Considering the widespread application of immune modulators, such as thymosin-α1 and bestatin, we explored the influence of these agents on the prognosis of HER2+ BRCA patients. Stratifying patients according to S100A9 intensity, we revealed that the long-term use of thymosin-α1 and bestatin both significantly improved the survival of patients with higher expression of S100A9, which might indicate beneficial response to adjuvant immunotherapy of HER2+ BRCA.

4.4. Potential of S100A9 as a novel marker of survival and therapeutic efficacy

S100A9, a kind of immunogenic protein, is an important inflammatory mediator which is widely involved in the occurrence, development, invasion and metastasis of malignant tumors. By comparison with physiological state, the overexpression of S100A9 is more obvious in malignant tumour tissues. The stability of S100A9 is poor due to the high risk of gene mutation such as chromosome deletion, translocation, and overlap in the coding region, which is proved to be closely related with progression of poorly differentiated

BRCA. More and more evidence shows that S100A9 could be considered as an effective marker of diagnosis and prognosis. In this study, we confirmed that overexpression of S100A9 inhibited anti-tumour immunological activity in the TME via promoting tumour cell metabolism. We also evaluated the correlation between S100A9 intensity and prognosis of HER2 positive BRCA cases. Further study will continue to supplement S100A9 as a novel marker of survival and therapeutic efficacy, providing potential target for immunological and metabolic therapy of BRCA.

4.5. Knowledge gaps in comparison to the newest studies and how to tackle them

Although we generally evaluated the immunogenicity of S100A9, the validity and reliability of our work still seemed to be insufficient. According to the currently published literature, we need to improve the further study in the following two aspects.

In terms of tissue samples, Pour and colleagues [49] conducted in-depth research via scRNA seq and flow cytometry and found that S100A9 intensity was contrary to the overall survival time in advanced melanoma patients. Inspired by this study, we propose to evaluate the effect of S100A9 on various immune cells in the TME by scRNA seq in subsequent studies. The relationship between S100A9 and infiltration of distinct immune cell subsets will also be estimated directly by multiple IHC assay.

In respect of in vivo models, Monteiro and colleagues [50] constructed brain metastasis model of lung cancer (H2030-BRM) and breast cancer (E0771-BRM), and demonstrated that S100A9 was the most significantly up-regulated gene in radiation resistant brain metastasis lesions. However, these two cell lines are very sensitive to radiotherapy when cultured *in vitro*, suggesting that TME may affect the therapeutic sensitivity of tumour cells. Enlightened by their work, appropriate animal model will be projected in the next step of our study, which would be conductive to verify the correlation between S100A9 and therapeutic sensitivity of HER2 positive BRCA.

4.6. Future development opportunity of immune therapy in the next 5 years

Currently, the existing treatment of BRCA nearly hit the bottleneck of their efficacy, which are incapable to improve overall survival of advanced BRCA substantially. TIL dominant cases of HER2 positive BRCA generally obtain better outcome, suggesting that the immunological therapy will become an essential treatment of this special population in the foreseeable future. Compared with other treatments, immune therapy aim to restore the immune surveillance by reversing the immune escape of tumour cells, thus improving the anti-tumour effect in the TME. Since the COVID-19 outbreak, research on immunology has obviously flourished, noting that immune therapy will usher in a rapid development. Hence the exploration of novel diagnostic and therapeutic targets will greatly improve the efficacy of personalized immune therapy, thereby being in keeping with the systemic therapy research topic of BRCA in the post-pandemic era.

4.7. Limitations

As a single-center clinical retrospective study, we are soberly aware of the shortcomings in our work. Regarding the limitations of single-center study, it could be argued that the reliability of this study depends on our experimental conditions, such as skill of researchers, equipment precision, reagent quality, culture environment of cell lines, and so on. Therefore, carrying out similar exploration in other centers would help to confirm the conclusions of our study. Another limitation of our work is validity deficiency, which is doomed by the characters of retrospective study. This limitation is apparent in many clinical research. Consequently, we have set about the next phage of our work and performed strictly control at the initial enrollment stage. We expect to prove our findings via multi-center prospective studies in the future.

Although widely accepted, bulk assays, such as QPCR, WB, and IHC, suffer from some limitations due to their deficiency in distinguishing various cell types. We then plan to explore more detailed tumour immune landscape of S100A9 anomalous cases via single cell RNA sequencing, thereby evaluating the effect of tumorigenic S100A9 expression on distinct subsets of immune cells in the TME. Moreover, this study was limited in the description of the distribution and proportion of TIL. Further research should be performed to explore the dynamic recruitment process of multifarious immune cell subsets. Despite the abundant evidence in tumour tissues, we have yet to establish proper models that could verify the relationship between the glycolysis-active phenotype and immune tolerance.

One more apparent limitation of our study is the sample size. Clearly hundred of samples are not enough to make generalizations about S100A9 related tumour metabolism and immune. However, from the results of those limited number, a clear pattern has emerged which highlighted the value of S100A9 as a novel prognostic marker of HER2 positive BRCA. Given the progression of natural course of HER2 positive BRCA, timely update of survival data will be attained from the consistently follow-up. Meanwhile, continuous improvement of statistical methods is necessary for us, and further survival analysis should be carried out according to the latest development of medical statistics.

5. Conclusions

The higher levels of S100A9 appeared to be a prominent and notable feature of HER2+ BRCA. Overexpression of S100A9 up-regulated the levels of the metabolic enzymes in tumour cells, which promoted TME acidification. These processes were largely due to the activation of the c-Myc-related pathway, which caused dephosphorylation and nuclear localisation of c-Myc, thus contributing to the elevated glycolytic activity. S100A9-related lactate accumulation also suppressed lymphocyte infiltration into the tumour stroma, the latter of which manifested as the scarce intensity of CD4+/CD8+ T cells and enrichment of FOXP3+ T cells.

Finally, the aberrant expression of S100A9 affected the efficacy of immune regulation agents and subsequently impaired the long-term survival of HER2+ BRCA cases.

Ethics statements

The authors agree to be accountable for all aspects of the work to ensure that questions related to the accuracy or integrity of any part of the work are appropriately investigated and resolved. The study was conducted in accordance with the Declaration of Helsinki (as revised in 2013). The study was approved by the Xiangya Hospital Ethics Committee (approved number 202004189) and individual informed consent for this study was in safe keeping.

Author contribution statement

Jia-qi Yuan: Conceived and designed the experiments; Performed the experiments; Analyzed and interpreted the data; Contributed reagents, materials, analysis tools or data; Wrote the paper.

Shouman Wang: Performed the experiments; Analyzed and interpreted the data; Contributed reagents, materials, analysis tools or data.

Lei Guo: Conceived and designed the experiments; Analyzed and interpreted the data; Contributed reagents, materials, analysis tools or data.

Funding statement

Dr. Jia-qi Yuan was supported by Wu Jieping Medical Foundation [320.6750.2020-20-28]; Health Commission of Hunan Province [202204082512]; Xiangya Hospital, Central South University [2209090555211]; Natural Science Foundation of Hunan Province [2022JJ70082].

Lei Guo was supported by Natural Science Foundation of Hunan Province [2022JJ30926].

Declaration of interest's statement

The authors declare that they have no known competing financial interests or personal relationships that could have appeared to influence the work reported in this paper.

Data availability statement

The raw data supporting the conclusions of this article will be made available upon request to interested researchers by the authors without undue reservation. Publication of all data did not compromise the anonymity of the participants or breach local data protection laws. Contact us via the corresponding author′s email to access to the data and material.

Publicly available datasets were analyzed in this study. These datasets can be found at the following sites:
http://www.gsea-msigdb.org/gsea/index.jsp,
https://kmplot.com/analysis/,http://gepia2.cancer-pku.cn/,
http://ualcan.path.uab.edu/, http://timer.cistrome.org/.

Authors made all codes available upon request to interested researchers. Contact us via the corresponding author′s email to access to the code.

Acknowledgments

The authors are grateful to Dr. Xue Dong and Dr. Shi-qin Liu for proofreading this manuscript.

Abbreviations

BRCA	Breast cancer
LPBC	Lymphocyte predominant breast cancer
TNBC	Triple negative breast cancer
DCIS	Ductal carcinoma in situ
LVSI	Lymph-vascular space invasion
pLN	Pathological-diagnosed lymph node metastasis
BCS	Breast-conserving surgery
ALND	Axillary lymph node dissection
SLNB	Sentinel lymph node biopsy
RT	Radiation therapy
TIL	Tumour infiltrating lymphocyte
MDSC	Myeloid derived suppressor cell

TME	Tumour micro-environment
DAMPs	Danger-associated molecular patterns
HER2	Human epidermal growth factor receptor 2
RAGE	Receptor for advanced glycation end products
TLR4	Toll-like receptor 4
S100A9	S100 calcium-binding protein A9
CD3	Cluster of differentiation 3 receptor
CD4	Cluster of differentiation 4 receptor
CD8	Cluster of differentiation 8 receptor
FOXP3	Forkhead/winged-helix transcription factor P3
LDHA	Lactate dehydrogenase A
PGK1	Phosphoglycerate kinase 1
ENO1	Enolase α
siRNA	Small interfering RNA transfection
RT-qPCR	Reverse transcription-quantitative polymerase chain reaction
WB	Western blotting assay
FISH	Fluorescence in situ hybridisation
IHC	Immunohistochemistry
H&E	Haematoxylin and eosin
SDS-PAGE	Sodium dodecyl sulphate-polyacrylamide gel electrophoresis
ECAR	Extracellular acidification rate
ROI	Region of interest
OD	Optical density
OCT	Optimal cutting temperature compound
HRP	Horseradish peroxidase
BCA	Bicinchoninic acid
2-DG	2-deoxyglucose
2-DG6P	2-deoxyglucose-6-phosphate
BSA	Bovine serum albumin
DAB	3, 3-diaminobenzidine tetrachloride
GSEA	Gene set enrichment analysis
NES	Normalised enrichment score
FDR	False discovery rate
Log_2FC	Log_2 fold change
HRs	Hazard ratios
CIs	Confidence intervals
ROC	Receiver operating characteristic
TCGA	The cancer genome atlas

Appendix A. Supplementary data

Supplementary data to this article can be found online at https://doi.org/10.1016/j.heliyon.2023.e13294.

References

[1] C.A. Hudis, Trastuzumab–mechanism of action and use in clinical practice, N. Engl. J. Med. 357 (2007) 39–51.
[2] L. Gianni, W. Eiermann, V. Semiglazov, et al., Neoadjuvant chemotherapy with trastuzumab followed by adjuvant trastuzumab versus neoadjuvant chemotherapy alone, in patients with HER2-positive locally advanced breast cancer (the NOAH trial): a randomised controlled superiority trial with a parallel HER2-negative cohort, Lancet 375 (2010) 377–384.
[3] D. Pectasides, A. Gaglia, P. Arapantoni-Dadioti, et al., HER-2/neu status of primary breast cancer and corresponding metastatic sites in patients with advanced breast cancer treated with trastuzumab-based therapy, Anticancer Res. 26 (2006) 647–653.
[4] S. Xu, H.R. Herschman, A tumor agnostic therapeutic strategy for hexokinase 1-null/hexokinase 2-positive cancers, Cancer Res. 79 (2019) 5907–5914.
[5] D. Hanahan, R.A. Weinberg, Hallmarks of cancer: the next generation, Cell 144 (2011) 646–674.
[6] A. Brand, K. Singer, G.E. Koehl, et al., LDHA-associated lactic acid production blunts tumor immunosurveillance by T and NK cells, Cell Metabol. 24 (2019) 657–671.
[7] M.C. Madonna, D.B. Fox, B.T. Crouch, et al., Optical imaging of glucose uptake and mitochondrial membrane potential to characterize Her2 breast tumor metabolic phenotypes, Mol. Cancer Res. 17 (7) (2019) 1545–1555.
[8] S.E. Stanton, S. Adams, M.L. Disis, Variation in the incidence and magnitude of tumor-infiltrating lymphocytes in breast cancer subtypes: a systematic review, JAMA Oncol. 2 (2016) 1354–1360.
[9] Karim Rihawi, Angela Dalia Ricci, Alessandro Rizzo, et al., Tumor-associated macrophages and inflammatory microenvironment in gastric cancer: novel translational implications, Int. J. Mol. Sci. 22 (8) (2021) 3805.
[10] Alessandro Rizzo, Angela Dalia Ricci, Biomarkers for breast cancer immunotherapy: PD-L1, TILs, and beyond, Expet Opin. Invest. Drugs 31 (6) (2022) 549–555.

[11] Angela Dalia Ricci, Alessandro Rizzo, Fabiola Lorena Rojas Llimpe, et al., Novel HER2-directed treatments in advanced gastric carcinoma: AnotHER paradigm shift? Cancers(Basel) 13 (7) (2021) 1664.
[12] K. Arai, T. Teratani, R. Kuruto-Niwa, et al., S100A9 expression in invasive ductal carcinoma of the breast: S100A9 expression in adenocarcinoma is closely associated with poor tumour differentiation, Eur. J. Cancer 40 (8) (2004) 1179–1187.
[13] S.S. Cross, F.C. Hamdy, J.C. Deloulme, et al., Expression of S100 proteins in normal human tissues and common cancers using tissue microarrays: S100A6, S100A8, S100A9 and S100A11 are all overexpressed in common cancers, Histopathology 46 (2005) 256–269.
[14] Y.I. Bao, A. Wang, J. Mo, S100A8/A9 is associated with estrogen receptor loss in breast cancer, Oncol. Lett. 11 (2016) 1936–1942.
[15] K. Arai, S. Takano, T. Teratani, et al., S100A8 and S100A9 overexpression is associated with poor pathological parameters in invasive ductal carcinoma of the breast, Curr. Cancer Drug Targets 8 (4) (2008) 243–252.
[16] M. Zhang, D. Chen, Z. Zhen, et al., Annexin A2 positively regulates milk synthesis and proliferation of bovine mammary epithelial cells through the mTOR signaling pathway, J. Cell. Physiol. 233 (2018) 2464–2475.
[17] P. Cheng, C.A. Corzo, N. Luetteke, et al., Inhibition of dendritic cell differentiation and accumulation of myeloid-derived suppressor cells in cancer is regulated by S100A9 protein, J. Exp. Med. 205 (10) (2008) 2235–2249.
[18] R. Salgado, C. Denkert, S. Demaria, et al., The evaluation of tumor-infiltrating lymphocytes (TILs) in breast cancer: recommendations by an International TILs Working Group 2014, Ann. Oncol. 26 (2015) 259–271.
[19] L. Zhou, X.D. He, Q.C. Cui, et al., Expression of LAPTM4B-35: a novel marker of progression, invasiveness and poor prognosis of extrahepatic cholangiocarcinoma, Cancer Lett. 264 (2008) 209–217.
[20] P. Cancemi, M. Buttacavoli, G. Di Cara, et al., A multiomics analysis of S100 protein family in breast cancer, Oncotarget 9 (2018) 29064–29081.
[21] S. Zhang, Z. Wang, W. Liu, et al., Distinct prognostic values of S100 mRNA expression in breast cancer, Sci. Rep. 7 (2017), 39786.
[22] R. Wu, L. Duan, L. Ye, et al., S100A9 promotes the proliferation and invasion of HepG2 hepatocellular carcinoma cells via the activation of the MAPK signaling pathway, Int. J. Oncol. 42 (3) (2013) 1001–1010.
[23] M. Huang, R. Wu, L. Chen, et al., S100A9 regulates MDSCs-mediated immune suppression via the RAGE and TLR4 signaling pathways in colorectal carcinoma, Front. Immunol. 10 (2019) 2243.
[24] S. Cheng, X. Zhang, N. Huang, et al., Down-regulation of S100A9 inhibits osteosarcoma cell growth through inactivating MAPK and NF-kappaB signaling pathways, BMC Cancer 16 (2016) 253.
[25] P. Gao, I. Tchernyshyov, T.C. Chang, et al., c-Myc suppression of miR-23a/b enhances mitochondrial glutaminase expression and glutamine metabolism, Nature 58 (2009) 762–765.
[26] Z.E. Stine, Z.E. Walton, B.J. Altman, et al., MYC, metabolism, and cancer, Cancer Discov. 5 (10) (2015) 1024–1039.
[27] J. Xu, Y. Chen, O.I. Olopade, MYC and breast cancer, Genes Cancer 1 (2010) 629–640.
[28] H. Zha, X. Li, H. Sun, et al., S100A9 promotes the proliferation and migration of cervical cancer cells by inducing epithelialmesenchymal transition and activating the Wnt/betacatenin pathway, Int. J. Oncol. 55 (2019) 35–44.
[29] A.A. Basiorka, K.L. McGraw, E.A. Eksioglu, et al., The NLRP3 inflammasome functions as a driver of the myelodysplastic syndrome phenotype, Blood 128 (2016) 2960–2975.
[30] L. Duan, R. Wu, L. Ye, et al., S100A8 and S100A9 are associated with colorectal carcinoma progression and contribute to colorectal carcinoma cell survival and migration via Wnt/beta-catenin pathway, PLoS One 8 (2013), e62092.
[31] B. Ruprecht, E.A. Zaal, J. Zecha, et al., Lapatinib resistance in breast cancer cells is accompanied by phosphorylation-mediated reprogramming of glycolysis, Cancer Res. 77 (2017) 1842–1853.
[32] S. Jain, X. Wang, C.C. Chang, et al., Src inhibition blocks c-Myc translation and glucose metabolism to prevent the development of breast cancer, Cancer Res. 75 (2015) 4863–4875.
[33] W.H. Fridman, J. Galon, F. Pagès, et al., Prognostic and predictive impact of intra- and peritumoral immune infiltrates, Cancer Res. 71 (2011) 5601–5605.
[34] S. Pilon-Thomas, K.N. Kodumudi, A.E. El-Kenawi, et al., Neutralization of tumor acidity improves antitumor responses to immunotherapy, Cancer Res. 76 (2016) 1381–1390.
[35] C.H. Chang, J. Qiu, D. O'Sullivan, et al., Metabolic competition in the tumor microenvironment is a driver of cancer progression, Cell 162 (2015) 1229–1241.
[36] C.H. Ottensmeier, K.L. Perry, E.L. Harden, et al., Upregulated glucose metabolism correlates inversely with CD8+ T-cell infiltration and survival in squamous cell carcinoma, Cancer Res. 76 (2016) 4136–4148.
[37] K. Renner, K. Singer, G.E. Koehl, et al., Metabolic hallmarks of tumor and immune cells in the tumor microenvironment, Front. Immunol. 8 (2017) 248.
[38] C.V. Dang, J.W. Kim, P. Gao, et al., The interplay between MYC and HIF in cancer, Nat. Rev. Cancer 8 (2008) 51–56.
[39] K. Tateishi, A.J. Iafrate, Q. Ho, et al., Myc-driven glycolysis is a therapeutic target in glioblastoma, Clin. Cancer Res. 22 (2016) 4452–4465.
[40] T. Schroeder, H. Yuan, B.L. Viglianti, et al., Spatial heterogeneity and oxygen dependence of glucose consumption in R3230Ac and fibrosarcomas of the Fischer 344 rat, Cancer Res. 65 (2005) 5163–5171.
[41] L. Ippolito, A. Morandi, E. Giannoni, et al., Lactate: a metabolic driver in the tumour landscape, Trends Biochem. Sci. 44 (2019) 153–166.
[42] T. Cascone, J.A. McKenzie, R.M. Mbofung, et al., Increased tumor glycolysis characterizes immune resistance to adoptive T cell therapy, Cell Metabol. 27 (2018) 977–987 e4.
[43] E. Gottfried, L.A. Kunz-Schughart, S. Ebner, et al., Tumor-derived lactic acid modulates dendritic cell activation and antigen expression, Blood 107 (2006) 2013–2021.
[44] M. Gallo, L. Sapio, A. Spina, et al., Lactic dehydrogenase and cancer: an overview, Front. Biosci. 20 (2015) 1234–1249.
[45] T. Imaoka, S. Yamashita, M. Nishimura, et al., Gene expression profiling distinguishes between spontaneous and radiation-induced rat mammary carcinomas, J. Radiat. Res. 49 (2008) 349–360.
[46] R. Kinoshita, H. Sato, A. Yamauchi, et al., Newly developed anti-S100A8/A9 monoclonal antibody efficiently prevents lung tropic cancer metastasis, Int. J. Cancer 145 (2019) 569–575.
[47] C. Sternberg, A. Armstrong, R. Pili, et al., Randomized, double-blind, placebo-controlled phaseIII study of tasquinimod in men with metastatic castration-resistant prostate cancer, J. Clin. Oncol. 34 (2016) 2636–2643.
[48] L. Shen, R. Pili, Tasquinimod targets suppressive myeloid cells in the tumor microenvironment, OncoImmunology 8 (2018), e1072672.
[49] Soudabeh Rad Pour, Yago Pico de Coaña, Xavier Martinez Demorentin, et al., Predicting anti-PD-1 responders in malignant melanoma from the frequency of S100A9+ monocytes in the blood, J. Immunother. Cancer 9 (5) (2021), e002171.
[50] Cátia Monteiro, Lauritz Miarka, María Perea-García, et al., Stratification of radiosensitive brain metastases based on an actionable S100A9/RAGE resistance mechanism, Nat. Med. 28 (4) (2022) 752–765.